

# Time-efficient frozen phonon multislice calculations for image simulations in high-resolution STEM

J. Barthel<sup>1</sup>

1. Ernst Ruska-Centre for microscopy and spectroscopy with electrons, Forschungszentrum Jülich and Aachen University, 52425 Jülich, Germany

ju.barthel@fz-juelich.de

Keywords: high-resolution STEM simulation, frozen phonon approximation, multislice calculations

A time-efficient implementation of the multislice algorithm [1] is applied including frozen phonon variations [2] in order to investigate how many frozen phonon states need to be considered to achieve a sufficiently good precision for a simulation of high-resolution scanning transmission electron microscopy (STEM) images. A small value of this simulation parameter would allow a minimum computation time for STEM images, which is frequently on the order of hours using conventional desktop computers. The investigated problem is related to the optimization of the number of calculated probe positions as discussed by Dwyer [3].

The implementation of the multislice algorithm applied here is using a set of  $M$  pre-calculated frozen phonon states for each of the  $N$  object structure slices. The object slices are chosen as thin as possible containing preferably only one atomic plane. Projected potentials are calculated using the parameterization of scattering factors by Weickenmeier and Kohl [4] including random atom displacements to represent thermal atom vibrations. During one run of the multislice calculation one of the  $M$  pre-calculated frozen states of the current slice is selected randomly and multiplied with the current wave function in form of a phase grating. A random permutation of the pre-calculated frozen states is produced by repeated application of this random selection scheme over the whole sample thickness. By this way one obtains free control over the number of frozen states applied to a scan pixel during run time without additional calculation effort. This scheme allows for example to adapt the number of averaged frozen states locally depending on the local signal variation and thereby to optimize the total calculation time in conjunction with an improved simulation precision. A fast run-time variation of frozen states requires a previous loading of all pre-calculated frozen states in form of phase-grating slices into the computer working memory. However, a large number of phase-grating pixels and frozen phonon states can be handled with commercially available computers supporting more than 4 Gigabytes working memory.

A minimum calculation time for a scan image is obtained by using only one random permutation of frozen slice states per scan pixel. As expected, this approach leads to a strong variation of the detected intensity per scan pixel. The intensity variation from pixel to pixel is visible in the upper row of Fig. 1 showing images composed of 40 x 40 scan pixels per projected SrTiO<sub>3</sub> [100] unit cell, where only one permutation of 25 unit cell periods from  $M = 50$  pre-calculated frozen states contributed to each scan pixel. A subsequent convolution of the images with an effective source profile is required to obtain qualitatively and quantitatively correct images [5]. The images of the lower row in Fig. 1 are obtained by convolution of the respective upper row images by a Gaussian source profile of 0.5 Å 1/e-half-width. The convoluted images appear smooth and represent also an average over frozen states applied to neighbour pixels within the effective source radius. This a-posteriori averaging of frozen states is possible due to a sufficiently small simulation scan step. In the present example, the scan step is approximately 10 pm per pixel, which is close to experimental scan steps frequently applied in high-resolution STEM. A sufficiently small scan step for a-posteriori frozen state averaging depends on the number of pixels per intensity peak in HAADF images before convolution and on the number of pixels within the effective source area for BF and ABF images.

Results of statistical evaluations from 90 independent calculations show a significant decrease of the pixel intensity variation after source profile convolution from approximately 40% down to 3% of the pixel mean value (see Fig. 1b). This precision level is sufficiently small for a comparison of simulation and experiment especially when analysing integrated column intensities. In conclusion, the consideration of just one frozen state per pixel is sufficient to obtain quantitatively meaningful simulation data when using realistic scan steps and subsequent source profile convolution.

## References

- [1] J.M. Cowley and A.F. Moodie, Acta Cryst. **10** (1957) p. 609.  
 [2] R.F. Loane, P. Xu, and J. Silcox, Acta Cryst. **A 47** (1991) p. 267.  
 [3] C. Dwyer, Ultramicroscopy **110** (2010) p. 195.  
 [4] A. Weickenmeier and H. Kohl, Acta Cryst. **A 47** (1991) p. 590.  
 [5] C. Dwyer, R. Erni, and J. Etheridge, Ultramicroscopy **110** (2010) p. 952.  
 [6] The author gratefully acknowledges funding from the German Ministry for Economics and Technology within the COORETEC initiative. A. Thust, M. Lentzen, L. Houben, and M. Heidelmann from the Ernst Ruska-Centre in Jülich are thanked for useful discussions.

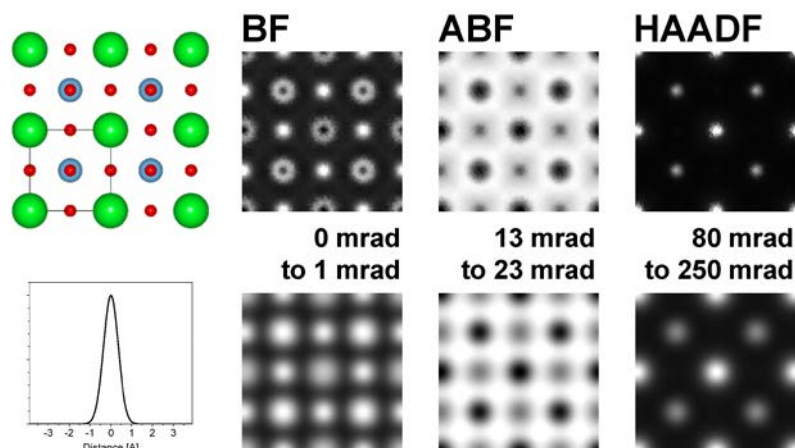


**Figure 1.** Model of  $2 \times 2$  unit cells of  $\text{SrTiO}_3$  in  $[100]$  projection (size  $7.81^2 \text{ \AA}^2$ ) with Sr at the unit cell corners, Ti in the center and O at the faces. Exemplary simulated aberration-free bright-field (BF), annular bright-field (ABF), and high-angle annular dark-field (HAADF) images for 300 kV electrons, 25 mrad illumination half-angle, and 10 nm object thickness using one frozen lattice permutation per pixel. Detection angles are noted next to the respective images. The images of the top row are obtained before convolution with the effective source profile, the lower row shows the same images after convolution. The applied Gaussian source profile is displayed below the projected structure model and scaled to the size of the images.

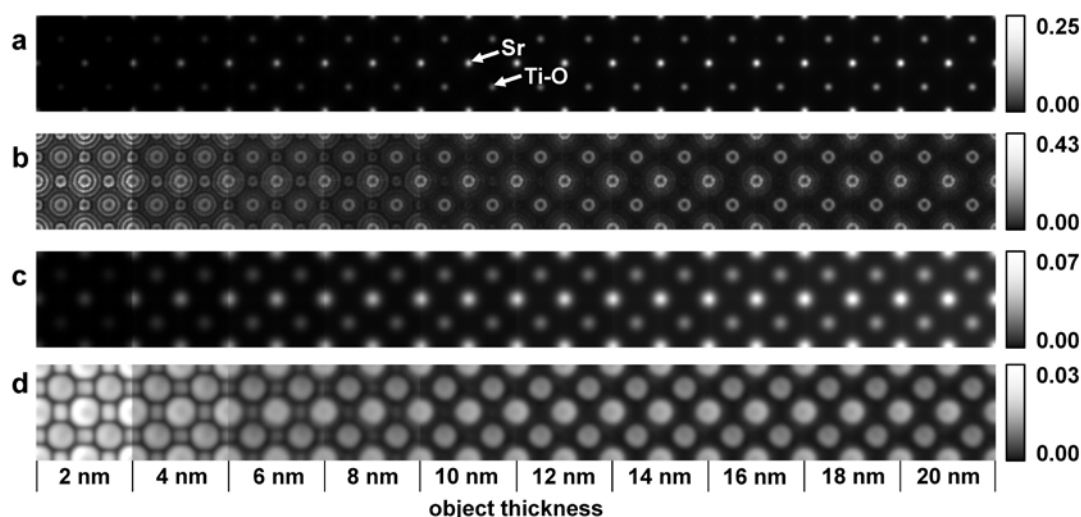


**Figure 2.** Series of simulated HAADF images of the same area and conditions as noted in Fig. 1 depending on object thickness. The images (a) and (c) show the average HAADF intensity of 90 statistically independent calculations relative to the incident probe intensity. Images (b) and (d) depict the standard deviation due to frozen lattice variations of the 90 calculations relative to the average intensities of (a) and (c) respectively. The upper two image series are obtained before source-profile convolution, whereas the lower image series are obtained with convoluted images. Respective white-level scales are noted to the right, and the object thickness of the  $2 \times 2$  unit cell patches is denoted below image (d).